ANTHROPOGENIC INFLUENCE ON THE HEAVIEST JUNE PRECIPITATION IN SOUTHEASTERN CHINA SINCE 1961

Ying Sun, Siyan Dong, Xuebin Zhang, Peter Stott, and Ting Hu

Anthropogenic influence has increased the chance of an extreme heavy precipitation event like that in June 2017 in southeastern China by about twofold, from a 0.6% probability to a 1.2% probability.

INTRODUCTION. In June 2017, southeastern China experienced heavy and long-lasting precipitation. The total precipitation amount was the highest on record since 1961 (Fig. 1) and was about 60% more than the 1961–90 average for June in the region. The normalized precipitation departure exceeds 3.0 sigma from the 1961–2017 mean. In Hunan province, which is located in central southeastern China, the persistent heavy rainfall at the end of June affected more than 7.8 million people, with 34 fatalities and about 0.8 million people displaced. The affected area of the crops was 605,000 hectares, with a total of 116,000 hectares without harvest. A total of 32,000 houses collapsed and 41,000 were severely damaged. The direct economic loss was 24.12 billion Chinese Yuan (CMA 2017; NCC 2017). It is therefore important to provide a timely answer as to the reasons for this heavy precipitation and if it is related to human influence.

AFFILIATIONS: Sun—National Climate Center, Laboratory for Climate Studies, China Meteorological Administration, Beijing, and Collaborative Innovation Center on Forecast and Evaluation of Meteorological Disasters, Nanjing University of Information Science and Technology, Nanjing, China; Dong and Hu—National Climate Center, Laboratory for Climate Studies, China Meteorological Administration, Beijing, China; Zhang—Climate Research Division, Environment and Climate Change Canada, Toronto, Ontario, Canada; Stott—Met Office Hadley Centre, Exeter, United Kingdom
CORRESPONDING AUTHOR: Ying Sun, sunying@cma.gov.cn

The abstract for this article can be found in this issue, following the table of contents.
DOI:10.1175/BAMS-D-18-0114.1

A supplement to this article is available online (10.1175/BAMS-D-18-0114.2).

Human-induced increases in greenhouse gases have contributed to the observed intensification of heavy precipitation events in many land areas (Zhang et al. 2007; Min et al. 2011; Zhang et al. 2013). Several studies have investigated the influence of external forcing on some heavy precipitation events in China (e.g., Zhou et al. 2013; Burke et al. 2016). In one case, human influence may have contributed to the occurrence probability of heavy precipitation in southeastern China in May (Burke et al. 2016) whereas in another case there was no clear evidence of human influence of heavy precipitation in northern China (Zhou et al. 2013). There is also evidence of human influence that results in a shift toward heavy precipitation over eastern China (Ma et al. 2017). Here, we use outputs from the large ensemble simulations conducted with the Canadian Earth System Model version 2 (CanESM2; Arora et al. 2011) to investigate possible human influence on heavy precipitation like the June 2017 precipitation event in southeastern China.

DATA AND METHODS. The precipitation event mainly covered the area 24°–32°N, 107°–124°E (box in Fig. 1). We use gauge observations of precipitation (SURF_CLI_CHN_MUL_DAY_V3.0; http://data.cma.cn/) that have been collected and rigorously quality controlled (Cao et al. 2016) at the China National Meteorological Information Center (NMIC). Since most Chinese stations were established after the late 1950s and the data become reliable and continuous after 1961, we use the station data in the region at about 600 stations for the period 1961–2017. We divide the region into multiple grid boxes at 2.8125° resolution, roughly consistent with the CanESM2 model grids. We average station precipitation amount within each grid. These gridded values are then averaged to obtain regional

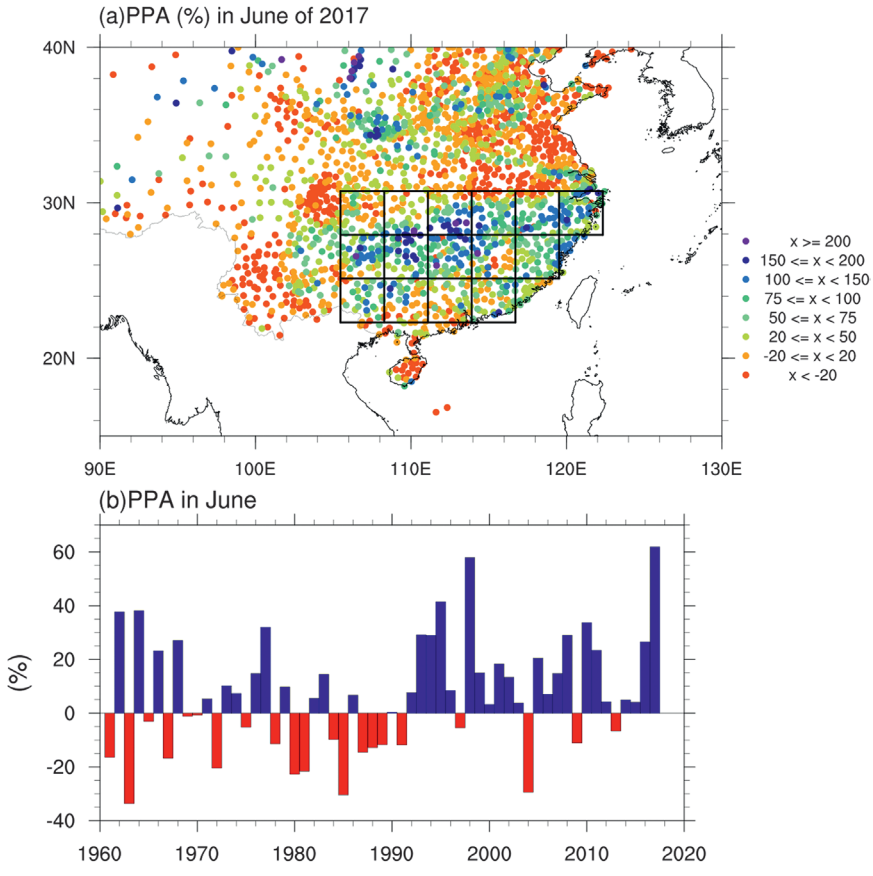

Fig. 1. Observed June percentage precipitation anomaly (PPA). (a) PPA (in percentage, relative to 1961–90 average) in June 2017 in China. The region defined as southeastern China is represented by the boxed areas. (b) Regional average of PPA in June in southeastern China during 1961–2017.

averages that are finally used to compute the percentage precipitation anomaly (PPA) relative to the 1961–90 base period.

CanESM2 was run at T63 resolution (~2.8° longitude/latitude) and included interactive atmosphere, ocean, sea ice, land, and carbon cycle components (Arora et al. 2011). Two large initial-condition ensembles, each consisting of 50 simulations, were randomly initiated from the conditions on 1 January 1950. Two sets of experiments forced with the historical anthropogenic (greenhouse gases combined with aerosols, land use changes, etc.) and natural forcing (ALL) and with natural forcing only (NAT) were conducted. The ALL experiments finished at the end of 2004 and the RCP8.5 scenario was used to extend the ALL simulations from January 2005 onward (Fyfe et al. 2017). The NAT experiments were driven by the solar and volcanic forcings from 1950 to 2020. The solar forcing for all years after 2005 replicated the forcing data from the last solar cycle observed before 2006 and there is no explosive volcanoes forcing after 2006.

The CanESM2 has a relatively high transient climate response (TCR) of 2.4°C (IPCC 2013), leading to higher global mean surface temperature (GMST) increase than the observations. To take this higher sensitivity into account and also make the results comparable with other models, we consider simulation over a 20-yr period (1992–2011) for which the CanESM2 simulated mean GMST is 1°C above the preindustrial level as simulated for the current climate. This is because Earth's surface has warmed about 1°C by 2017. In the following, the event probabilities in model simulations are computed based on data from the period of 1992–2011.

Our analyses include the following steps: 1) Compute the regional percentage precipitation anomaly (PPA) in June for observations and for individual ALL and NAT forcing runs during 1961–2017. 2) Estimate the probability (P_{OBS}) for the observed June 2017 precipitation in the observational data using an empirical probability formula (Bonsal et al. 2001). This method is easy to implement and does not assume a probability distribution for the data. 3) Pool the 51 years (1950–2000) of data that occur before GMST rises by 1°C from each of the 50 ALL runs together and then estimate the PPA magnitude (PPA_{ALL}) in the pooled data corresponding to the event probability P_{OBS}, using the same probability formula. 4) Pool the 20 years (1992–2011) of data corresponding to the current climate from each of the 50 NAT runs and then estimate the probability of PPA_{ALL} in NAT simulations (P_{NAT}). 5) Compute the risk ratio $RR = P_{ALL}/P_{NAT}$. 6) Use a bootstrap method to estimate the confidence interval of the risk ratio. This involves three steps: (a) draw 50 samples of 57-yr data from the 50 ALL runs with replacement and then compute PPA_{ALL}; (b) draw 50 samples of 20 years of data from the 50 NAT runs with replacement and then compute P_{NAT}; and (c) compute risk ratio from the bootstrapped samples and repeat the bootstrap

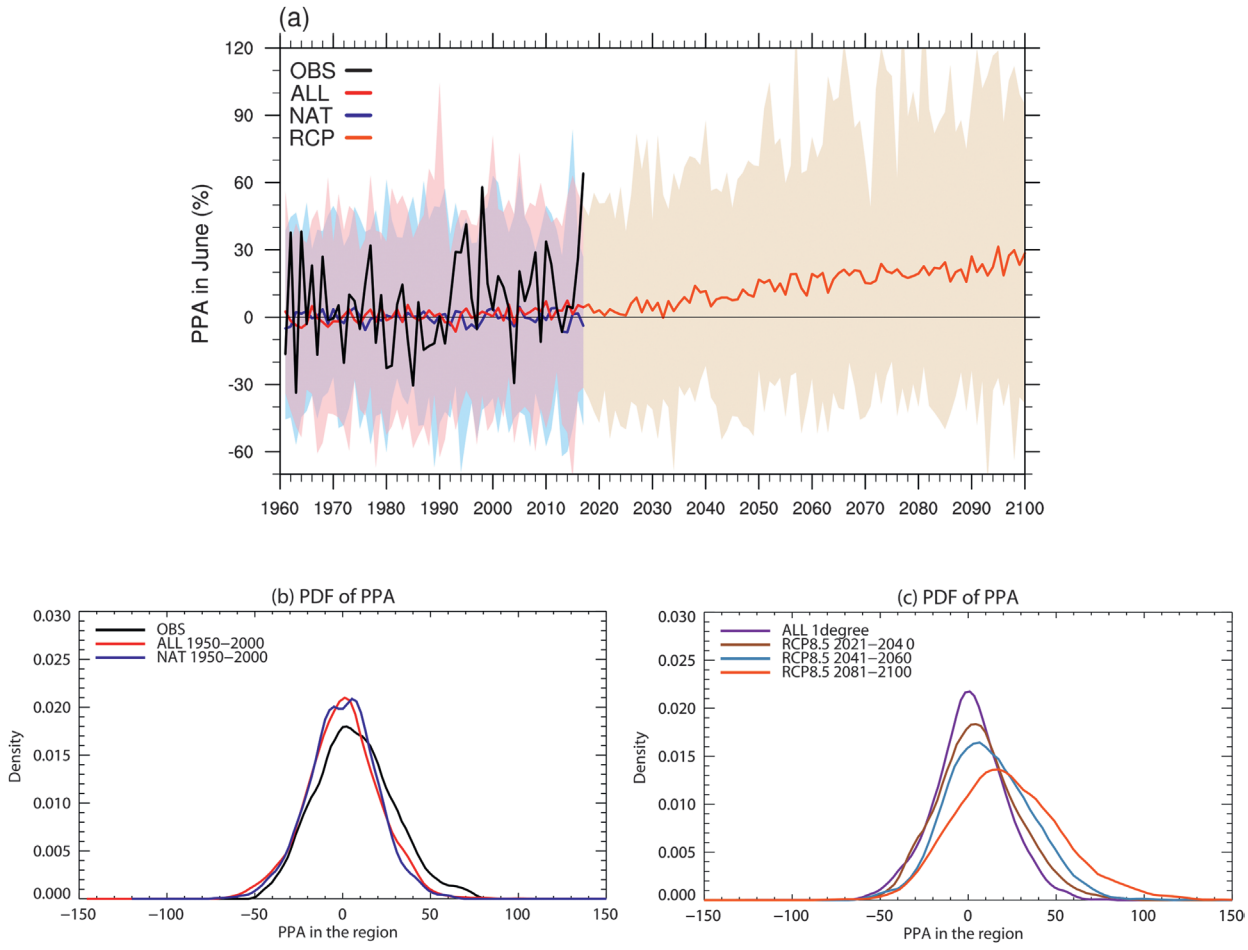

Fig. 2. Observed and simulated regional precipitation anomaly in June and relevant statistics. (a) Observed and simulated PPA for southeastern China. The black line shows the observations while the red, blue, and orange lines display the multimodel ensemble mean under ALL, NAT, and RCP8.5 forcings, respectively. Shadings indicate the ensemble spread by the 50 members. (b) Histograms of observed (black) and simulated percentage precipitation anomalies for 1961–2017 driven by ALL (purple) and NAT (blue) forcings. (c) Histograms of percentage precipitation anomaly simulated by CanESM2 under ALL (red) and RCP8.5 scenario for the future periods in 2021–40 (brown), 2041–60 (light blue), and 2081–2100 (orange).

procedure 1000 times. For the future climate under RCP8.5 scenario, the three time periods 2021–40, 2041–60, and 2081–2100 are selected to compute the occurrence probability of the events like 2017 PPA_{ALL}. The P_{RCP} can be obtained with the same method as the probability calculation P_{NAT}. Then the risk ratios for future climate are calculated as compared with the climate without anthropogenic forcing under NAT forcing (P_{RCP}/P_{NAT}) and with the current observational world (P_{RCP}/P_{OBS}).

RESULTS. Figure 1a shows that the June 2017 anomalous heavy precipitation was centered in southeastern China, especially in the region south of the Yangtze River Valley. Other areas in China experienced below-normal precipitation during this month. In the studied region, the percentage precipitation anomaly in many stations (135 stations; 22% in the studied region) is higher than 100% with some stations experiencing a record-breaking amount of precipitation. The three stations with the highest June PPA (233%, 217%, and 210%) were all located in Hunan Province, where the most serious flooding disaster caused various problems for human life and society. Figure 1b shows the regional mean series for southeastern China. It is apparent that June has been very wet since the early 1990s and the June 2017 was the wettest since 1961, with a PPA_{OBS} value of 61.9%. The probability for a 2017-like event is 1.2% ($P_{OBS} = 0.012$) in the observational data, which corresponds to 1-in-83-yr event. The second largest PPA_{OBS} occurred in 1998 with a PPA value of 57.9%.

Figure 2a shows the observed (black) and simulated June precipitation anomalies under ALL (red), NAT

(blue), and RCP8.5 (orange) in southeastern China in 1961–2017 and the years after 2018 till 2100. The simulated June precipitation amount 164.6 mm (157.1–172.7 mm; Fig. ES1) is smaller than the observation (247.4 mm), but the standard deviation of June precipitation in the simulation (20.5 mm, with a 5%–95% range of 18.4–22.9 mm) is more comparable with the observed one (20.9 mm). This means that the normalized PPA would have slightly larger variations in the models than those observed. Figure 2a shows that the model results under ALL and NAT forcings cover the observed range. The ensemble mean values under ALL and NAT forcing are small, suggesting that the response of precipitation to external forcing is still very small compared with the natural internal variability. Figure 2b shows the PDF distribution of observed and simulated PPA. The observed data slightly skew rightward but this cannot be seen in the models. For the observed 2017-like event probability $P_{OBS} = 0.012$, the corresponding PPA magnitude under ALL forcing (PPA_{ALL}) is 46.5% [90% confidence interval (CI): 44.3%–52.3%]. The probability of a PPA of 46.5% under NAT forcing is 0.6% ($p = 0.006$) (90% CI: 0.003–0.011), which is a 1-in-172.4-yr event (90% CI: 92.9–369.1 yr). Correspondingly, we can estimate that the risk ratio (RR) is 2.1 (90% CI: 0.9–6.8), indicating that human-induced climate change may have increased the probability of a 2017-like event by about twofold.

Under the future RCP8.5 scenario, the ensemble mean of regional percentage precipitation anomalies simulated by CanESM2 show a clear increasing trend (Fig. 2a). Additionally, the PDFs of PPA in the early (2021–40), middle (2041–60), and late twenty-first century (2081–2100) clearly shift rightward (Fig. 2c). The distribution becomes wider and shorter compared with the observation, especially in 2081–2100. The probabilities of PPA_{ALL} in three future stages are 0.044 (90% CI: 0.033–0.057), 0.088 (90% CI: 0.072–0.103), and 0.195 (90% CI: 0.177–0.217), respectively. These correspond to 1-in-22.6-yr (90% CI: 17.3–30.9 yr), 1-in-11.3-yr (90% CI: 9.6–13.8 yr), and 1-in-5.1-yr (90% CI: 4.5–5.6 yr) events. Compared with the NAT experiments, the estimated risk ratios are 7.6 (90% CI: 3.1–26.6), 15.2 (90% CI: 6.3–51.1), and 33.8 (90% CI: 14.6–111.6). If we compare the increased probability of such an event with those that occurred in the current observational world (P_{OBS}), the risk ratio would be 3.7 (90% CI: 2.7–4.8), 7.3 (90% CI: 6.0–8.7), and 16.3 (90% CI: 14.7–18.2) under the influence of future increased human activities. All these indicate that the occurrence risk of 2017-like events will increase with the increased anthropogenic forcing. As CanESM2 has larger sensitivities, the projected changes would be larger than median projection by CMIP5 models. The projected changes would also be less under other RCP scenarios with various mitigation efforts such as RCP4.5 or RCP2.6.

CONCLUSIONS. The human influence on the heaviest June precipitation since 1961 in southeastern China is analyzed with the observational and CanESM2 model data. The results show that the probability of extreme June precipitation that is as rare as or rarer than the June 2017 event in the ALL simulations has increased by about twofold when compared with the NAT simulations. This indicates that the anthropogenic influence may have increased the chance for such an event happening. Additionally, the model suggests that increases in regional precipitation will become more likely and probabilities for a similar event are projected to increase progressively more with future anthropogenic warming. These future projections provide additional support for the conclusion that the occurrence probability of such heavy precipitation may already be increasing due to human influence.

ACKNOWLEDGMENTS. Y.S., S. D., and T. H. are supported by China funding agencies through multiple grants: China 2018YFA0605604, NSFC 41675074 and 41775082, and CCSF201805. PAS was supported by the UK–China Research and Innovation Partnership Fund through the Met Office Climate Science for Service Partnership (CSSP) China as part of the Newton Fund, the EUCLEIA project funded by the European Union's Seventh Framework Programme (FP7/2007–13) under Grant Agreement 607085, and the Joint UK DECCBEIS/Defra Met Office Hadley Centre Climate Programme (GA01101).

REFERENCES

Arora, V. K., and Coauthors, 2011: Carbon emission limits required to satisfy future representative concentration pathways of greenhouse gases. *Geophys. Res. Lett.*, **38**, L05805, https://doi.org/10.1029/2010GL046270.

Bonsal, B. R., X. Zhang, L. A. Vincent, and W. D. Hogg, 2001: Characteristics of daily and extreme temperatures over Canada. *J. Climate*, **14**, 1959–1976, https://doi.org/10.1175/1520-0442(2001)014<1959:CODAET>2.0.CO;2.

Burke, C., P. Stott, Y. Sun, and A. Ciavarella, 2016: Attribution of extreme rainfall in South East China during May 2015 [in "Explaining Extremes of 2015 from a Climate Perspective"]. *Bull. Amer. Meteor. Soc.*, **97**, S92–S96, https://doi.org/10.1175/BAMS-D-16-0144.1.

Cao, L., Y. Zhu, G. Tang, F. Yuan, and Z. Yan, 2016: Climatic warming in China according to a homogenized

data set from 2419 stations. *Int. J. Climatol.*, **36**, 4384–4392, https://doi.org/10.1002/joc.4639.

CMA, 2017: China Climate Bulletin 2017 (in Chinese with English abstract). China Meteorological Administration, 54 pp., www.cma.gov.cn/root7/auto13139/201801/t20180117_460484.html.

Fyfe, J. C., and Coauthors, 2017: Large near-term projected snowpack loss over the western United States. *Nat. Commun.*, **8**, 14996, https://doi.org/10.1038/ncomms14996.

IPCC, 2013: *Climate Change 2013: The Physical Science Basis*. T. F. Stocker et al., Eds., Cambridge University Press, 1535 pp.

Ma, S., and Coauthors, 2017: Detectable anthropogenic shift toward heavy precipitation over eastern China. *J. Climate*, **30**, 1381–1396, https://doi.org/10.1175/JCLI-D-16-0311.1.

Min, S.-K., X. B. Zhang, F. W. Zwiers, and G. C. Hegerl, 2011: Human contribution to more-intense precipitation extremes. *Nature*, **470**, 378–381, https://doi.org/10.1038/nature09763.

NCC, 2017: China Monthly Climate Bulletin for June 2017. National Climate Center of China Meteorological Administration, 18 pp, http://cmdp.ncc-cma.net/influ/moni_china.php.

Zhang, X., F. W. Zwiers, G. C. Hegerl, F. H. Lambert, N. P. Gillett, S. Solomon, P. Stott, and T. Nozawa, 2007: Detection of human influence on twentieth-century precipitation trends. *Nature*, **448**, 461–465, https://doi.org/10.1038/nature06025.

——, H. Wan, F. W. Zwiers, G. C. Hegerl, and S.-K. Min, 2013: Attributing intensification of precipitation extremes to human influence. *Geophys. Res. Lett.*, **40**, 5252–5257, https://doi.org/10.1002/grl.51010.

Zhou, T. J., F. F. Song, R. P. Lin, X. L. Chen, and X. Y. Chen, 2013: The 2012 North China floods: Explaining an extreme rainfall event in the context of a longer-term drying tendency [in "Explaining Extreme Events of 2012 from a Climate Perspective"]. *Bull. Amer. Meteor. Soc.*, **94**, S49–S51, https://doi.org/10.1175/BAMS-D-13-00085.1.